https://doi.org/10.5194/egusphere-2026-2303
Preprint. Discussion started: 27 May 2026

Improving photosynthate allocation dynamic simulations of crops under water stress conditions

Wei Xu[a,b], Wen Zhang[a], Yongqiang Yu[a], Qing Zhang[a,*]

[a] Laboratory of Atmospheric Boundary Layer, Institute of Atmospheric Physics, Chinese Academy of Sciences, Beijing 100029, China
[b] College of Earth and Planetary Sciences, University of Chinese Academy of Sciences, Beijing 100029, China
Email address: zhangqing@mail.iap.ac.cn

Abstract

Accurately simulating crop photosynthate allocation under water stress is critical for predicting both food security and ecosystem carbon sequestration (SOC inputs). Current crop models often rely on static or growth-stage-fixed partitioning coefficients, which limits their ability to capture the physiological plasticity of crops responding to fluctuating environmental conditions. This study develops a water-driven, stage-dependent carbon allocation scheme within the Agro-C model to better represent crop responses to soil moisture variability. The scheme dynamically adjusts photosynthate partitioning coefficients for roots (PR) and leaves (PL), integrates the yellow-to-green leaf ratio (YGR), and incorporates a water stress–induced leaf senescence module. By linking carbon allocation to both soil moisture and crop development, the approach improves the representation of physiologically regulated allocation processes and enhances the realism of crop simulations. Model evaluation using extensive datasets for maize and wheat demonstrates substantial improvements in simulation accuracy, with R^2 values reaching 0.77–0.95 for aboveground biomass (AGB) and 0.62–0.83 for belowground biomass (BGB). These results underscore the importance of dynamically representing carbon allocation under water stress and offer an improved framework for simulating carbon–water interactions in agroecosystems.

Key words: Crop model, Water stress, Irrigation, photosynthate allocation

https://doi.org/10.5194/egusphere-2026-2303
Preprint. Discussion started: 27 May 2026

1. Introduction

The intensification of climate change and increasing pressure on freshwater resources have led to more frequent and severe drought events worldwide (Boretti & Rosa, 2019; Lesk et al., 2016; Vicente-Serrano et al., 2022). Water availability is a key factor regulating crop growth and productivity, as sufficient water promotes biomass accumulation and yield, whereas water deficit can cause substantial reductions (Zlatev & Lidon, 2012). Beyond its direct effects on crop growth, water stress fundamentally alters the allocation of assimilated carbon among plant organs, thereby influencing both plant development and soil carbon inputs.

Maize (*Zea mays L.*) and wheat (*Triticum spp.*), as major global staple crops, are highly sensitive to water availability (Hu et al., 2024; Yan et al., 2025). Under drought conditions, crops dynamically adjust carbon allocation to optimize resource acquisition. Moderate water deficit may promote root growth and enhance water use efficiency by increasing carbon allocation belowground (Chen et al., 2019; Oktem, 2008), whereas severe drought suppresses carbon assimilation and reduces both aboveground and belowground biomass, ultimately limiting yield formation (Khatun et al., 2021; Li et al., 2021). In wheat, drought responses are stage-dependent, with increased root allocation under mild stress but inhibited root development under severe water deficit (Wang et al., 2024; Xue et al., 2003). In contrast, excessive water conditions such as waterlogging can impair root function and disrupt carbon allocation patterns (Manghwar et al., 2024). Although recent studies have quantified relationships between water availability and biomass allocation (Xu et al., 2025), incorporating these dynamic responses into crop models remains a major challenge.

Photosynthate partitioning is a key process linking carbon assimilation to vegetation growth in terrestrial ecosystem models, yet it is typically represented using empirical, fixed, or stage-based partitioning schemes (Hijmans et al., 1994; Wolf et al., 2003). In the Agricultural Production Systems sIMulator (APSIM), assimilate partitioning among organs is regulated by developmental stage, with carbon allocated to leaves during early growth and progressively shifted to stems, reproductive organs,

https://doi.org/10.5194/egusphere-2026-2303
Preprint. Discussion started: 27 May 2026

and grains (Keating et al., 2003). The Carnegie–Ames–Stanford Approach model (CASA) (Field et al., 1995) and the Denitrification-Decomposition (DNDC) model (Li et al., 2011), biomass partitioning is largely based on fixed parameters, with the root to shoot ratio (RSR) varying only by vegetation type. In reality, assimilate partitioning is a highly flexible process that responds to changing resource availability, particularly soil moisture conditions, and plays a critical role in regulating both plant growth and soil carbon input. Therefore, developing a mechanistic representation of photosynthate allocation that explicitly accounts for environmental controls is essential for improving model accuracy and physiological realism (Hu et al., 2023).

Moreover, the impacts of water deficit on crops involve multiple aspects of plant growth and development, and it remains challenging to quantitatively and precisely describe water stress in crop models. Most crop models use a water stress coefficient (K_s) based on supply–demand balance to adjust assimilate allocation and estimate biomass under stress (Saseendran et al., 2014). For instance, in the APSIM (McCown et al., 1996), CropSyst (Stöckle et al., 1994), and Decision Support System for Agrotechnology Transfer (DSSAT) (Jones et al., 2003), the water stress coefficient is defined as $K_s = 1 - AT / PT$, where AT is the actual daily water uptake and PT is the potential transpiration. When soil water supply is insufficient to meet the crop's transpiration or evapotranspiration demand, the plant experiences water stress.

However, in reality, crop water supply primarily depends on root water uptake from the soil (Steudle, 2000). Water transport within the plant is driven by the water potential gradient along the soil–plant–atmosphere continuum, which sustains plant water status and transpiration. Root water uptake is governed not only by the water potential gradient between soil and roots, but also by root hydraulic conductivity. Thus, plant water uptake capacity is jointly determined by these above two factors (Wang et al., 2005; Wang et al., 2013; Yang et al., 2023). In addition, root system architecture, root length density, and the spatial distribution of soil moisture further influence the efficiency of water acquisition, thereby regulating plant water status and its response to water stress (Javaux et al., 2008). Hence, incorporating root water

https://doi.org/10.5194/egusphere-2026-2303
Preprint. Discussion started: 27 May 2026

uptake processes provides a more physiologically meaningful basis for representing water stress in crop models.

Therefore, to address current limitations in modeling crop responses to varying water availability, this study optimizes the Agro-C model—a biogeophysical framework for simulating crop growth and SOC dynamics (Huang et al., 2009; Yu et al., 2012; Wang et al., 2015; Zhang et al., 2017). Specifically, we replace its conventional stage-dependent partitioning strategy with a newly developed, moisture-driven dynamic allocation scheme. Focusing on maize and wheat as representative C4 and C3 crops, we aim to: (1) quantify the non-linear responses of leaf and root partitioning coefficients (PL and PR) to soil water availability while incorporating a drought-induced leaf senescence module (YGR) to represent declines in photosynthetic capacity; (2) improve the water module of the Agro-C model by integrating root water uptake characteristics, allowing water stress to be represented based on crop physiological responses; and (3) validate the model's performance in capturing carbon trade-offs under extreme water regimes.

2. Methods and materials

2.1 Data Sources

Up on the datasets used for the meta-analysis by Xu et al. (2025), we further screened studies for model calibration and validation by the following criteria: (i) the study must report belowground biomass (BGB) or aboveground biomass (AGB) for one or more crop growth stages; (ii) the study must provide irrigation amounts or soil moisture conditions throughout the crop growth period; (iii) the study must report fertilizer inputs during the cropping period; and (iv) background and ancillary information such as geographic coordinates, altitude, planting area, planting density, soil type, and bulk density must be described. Meteorological data for the crop growing period were obtained from *ERA5* (https://cds.climate.copernicus.eu/).

Totally we collected 608 observations of AGB and BGB (315 for maize and 293 for wheat) from 21 published studies, including 198 at maturity and 411 at earlier

https://doi.org/10.5194/egusphere-2026-2303
Preprint. Discussion started: 27 May 2026

115 developmental stages. In 12 studies (maize: 214, wheat: 164), AGB and BGB were
116 recorded at multiple key growth stages, and these data were used for model
117 calibration. In contrast, 9 studies (maize: 101, wheat: 129) reported AGB and BGB
118 only at maturity or vegetative stages, and these data were used for model validation.
119 The geographic distribution of the dataset is shown in Fig. S1.

120 2.2 Simulations of the crop growth responses to and the budgets of soil water
121 conditions in Agro-C model

122 In Agro-C model, Huang et al. (2009) simulated soil water content based on the
123 principle of soil water balance, using precipitation and actual evapotranspiration at the
124 canopy level. The effects of soil water on photosynthesis were represented as follows:

125 $$F_{w(i)} = \begin{cases} 0 & W_{(i)} \le W_p \\ \frac{W_{(i)} - W_p}{W_l - W_p} & W_p < W_{(i)} < W_l \\ 1 & W_l < W_{(i)} \le W_u \\ 0.5 \times (1 + \frac{W_{(i)} - 1}{W_u - 1}) & W_{(i)} \ge W_u \end{cases} \quad (1)$$

126 where W_p represents the soil water content at the wilting point ($cm^{-3} \cdot cm^{-3}$), while W_l
127 and W_u denote the lower and upper limits of optimal soil water content ($cm^{-3} \cdot cm^{-3}$),
128 respectively. $W_{(i)}$ is the daily mean soil water content in the 0–40 cm layer ($cm^{-3} \cdot cm^{-3}$).
129 The daily soil moisture $W_{(i)}$ is calculated by balancing precipitation and actual
130 evapotranspiration, as expressed in the following equation:

131 $$W_{(i)} = W_{(i)-1} + \frac{PRE_i - EA_i}{h} \quad (2)$$

132 PRE_i and EA_i represent daily precipitation (mm) and evapotranspiration (mm),
133 respectively, while h denotes soil depth (mm). We assumed that precipitation is
134 retained within the 0–40 cm soil layer, neglecting runoff and vertical percolation.
135 Evapotranspiration was determined jointly by the leaf area index (LAI) and potential
136 evapotranspiration (ET_0) (Ritchie, 1998). ET_0 was calculated using the
137 Priestley–Taylor equation (Priestley and Taylor, 1972).

138 In simulating vegetation photosynthesis, the Agro-C model does not account for

https://doi.org/10.5194/egusphere-2026-2303
Preprint. Discussion started: 27 May 2026

water stress. Instead, the model determines whether irrigation is required by calculating the difference between soil water content (SWC) and the thresholds defined by the wilting point (W_P) and field capacity (FC).

$$W_{diff} = W_{(i)} - ((W_{FC} - W_p) \times 0.5 + W_p) \quad (3)$$

where W_{FC} represents the field capacity ($cm^{-3} \cdot cm^{-3}$). When $W_{diff} < 0$, the crop is considered to require irrigation. The irrigation method is defined as follows:

$$W_{(i)} = \frac{(W_{(i)} + 100)}{h} \quad (4)$$

2.3 Modelling adjustments of the water dynamics and the responsive crop assimilates partitioning

In the optimized Agro-C model, crop water stress was determined by calculating the difference ($\Delta W_{(i)}$, mm) between the daily crop water requirement (ET_c, mm) and the actual daily water uptake ($W_{u,(i)}$, mm).

$$\Delta W_{(i)} = ET_{c,(i)} - W_{u,(i)} \quad (5)$$

When $\Delta W_{(i)} > 0$, drought stress exists; when $\Delta W_{(i)} < 0$, the crops require sufficient water.

ET_c is calculated based on crop evapotranspiration and crop coefficient (K_c) :

$$ET_c = K_c \times ET_0 \quad (6)$$

The K_c values at different growth stages were derived from *FAO-56* (Allen et al., 2005).

Roots are the primary organs for water and nutrient acquisition. The root water uptake rate per unit volume of soil $W_{u,(i)}$ ($m^3 \cdot m^{-3} \cdot s^{-1}$) is driven by the water potential gradient between the soil and the root xylem, and regulated by the root hydraulic conductivity of that layer ($C_{r,(i)}$, $s^{-1} \cdot MPa^{-1}$) (Hafner et al., 2020).

$$W_{u,(i)} = \Delta\psi_{(i)} \times C_{r,(i)} \quad (7)$$

The root-soil water potential difference $\Delta\psi_{(i)}$ is primarily determined by the

https://doi.org/10.5194/egusphere-2026-2303
Preprint. Discussion started: 27 May 2026

dynamics of $\psi_{s,(i)}$(MPa), as plants tend to maintain $\psi_{r,(i)}$ (MPa) within a relatively stable range through osmoregulation (Dodd et al., 2010). For model simplification under well-watered conditions, $\psi_{r,(i)}$ can be treated as an empirical constant derived from literature (Munns and Tester, 2008; Novák et al., 2005).

$$\Delta\psi_i = (\psi_{s,(i)} - \psi_{r,(i)}) \quad (8)$$

The root hydraulic conductivity ($C_{r,(i)}$) represents the water flux from a unit volume of soil per unit water potential gradient. It is calculated as the product of the total root surface area in that soil volume and the intrinsic hydraulic conductance per unit root surface area (Lp_r $m \cdot s^{-1} \cdot Mpa^{-1}$).

$$C_{r,i} = (M_{r,i-1} \times S_r) \times Lp_r \quad (9)$$

where $M_{r,(i-1)}$ is the root dry mass per unit soil volume ($g \cdot m^{-3}$), S_r is the specific root surface area ($m^2 \cdot g^{-1}$). To avoid circular dependency and ensure numerical stability, root water uptake ($W_{u,(i)}$) was calculated using root biomass from the previous time step. The term ($M_{r,(i-1)} \times S_r$) thus gives the root surface area density. Values of Lp_r for maize (Steudle, 2000; Cai et al., 2022; Rishmawi et al., 2023; Protto et al., 2024) and wheat (Cai et al., 2022; Yang et al., 2023) at different developmental stages were obtained from the literature.

2.4 Calibration of photosynthate partitioning coefficients in Agro-C model

In the Agro-C model, the crop development index (DVI) is defined as 0 at emergence, 1 at heading for wheat or silking for maize, and 2 at maturity. The DVI is divided into 21 intervals at increments of 0.1. Within each interval, the proportion of assimilates allocated to leaves (PL) and roots (PR) is fixed (Huang et al., 2009), while the proportion allocated to stems is calculated as 1- (PL + PR). During the vegetative growth stage, the allocation of dry matter to roots and leaves decreases with development, whereas during the reproductive stage, all assimilates are allocated exclusively to grains (Table S1).

https://doi.org/10.5194/egusphere-2026-2303
Preprint. Discussion started: 27 May 2026

Jiang et al. (2018) demonstrated that under water stress, the assimilate partitioning ratios to roots, stems, and leaves all vary with water availability. Therefore, in the Agro-C model, the pre-optimized partitioning ratios for leaves and roots need to be appropriately adjusted ($\Delta PL_{(i)}$ and $\Delta PR_{(i)}$) to enable the model to capture assimilate allocation mechanisms under different water conditions. The calibrated partitioning coefficients for leaves and roots ($PL_{N(i)}$ and $PR_{N(i)}$) are thus obtained by adding the adjustment terms to the pre-optimized coefficients ($PL_{O(i)}$ and $PR_{O(i)}$).

$$PL_{N(i)} = PL_{O(i)} + \Delta PL_{(i)} \quad (10)$$

$$PR_{N(i)} = PR_{O(i)} + \Delta PR_{(i)} \quad (11)$$

In the initial stage of model calibration, before clarifying the relationships of $\Delta PL_{(i)}$ and $\Delta PR_{(i)}$ with water availability, constant values of $\Delta PL_{(i)}$ and $\Delta PR_{(i)}$ were preliminarily assigned. The feasibility of these values was then evaluated by comparing the simulated aboveground and belowground biomass (Sim_AGB, Sim_BGB) with the observed values (Obs_AGB, Obs_BGB). If both ratios Sim_AGB / Obs_AGB and Sim_BGB / Obs_BGB exceeded 80%, the assigned $\Delta PL_{(i)}$ and $\Delta PR_{(i)}$ were considered acceptable (Fig. 1).

After the initial calibration of the model, correlation equations between $\Delta PL_{(i)}$, $\Delta PR_{(i)}$, and $\Delta W_{(i)}$ were developed. These equations were then used to replace the initially assigned constant values, thereby providing a more accurate and explicit representation of the changes in assimilate partitioning coefficients under soil water stress.

Drought stress accelerates leaf senescence, abscission, and mortality, thereby altering the yellow-to-green leaf ratio (YGR) (Seleiman et al., 2021). In addition to calibrating the assimilate partitioning coefficients, we also adjusted the YG_R parameter in the pre-optimized Agro-C model. Specifically, correlation equations between the increment of the yellow-to-green leaf ratio ($\Delta YGR_{(i)}$) and $\Delta W_{(i)}$ were developed to represent the calibrated YGR ($YGR_{N(i)}$) under dynamically varying soil

https://doi.org/10.5194/egusphere-2026-2303
Preprint. Discussion started: 27 May 2026

water conditions.

$$YGR_{N(i)} = YGR_{O(i)} + \Delta YGR_{(i)} \quad (12)$$

where $YGR_{O(i)}$ represents the yellow-to-green leaf ratio in the pre-optimized Agro-C model.

To simplify the model, we further incorporated the DVI as an additional independent variable in the above equations, thereby accounting for the combined effects of water availability and crop developmental stage on assimilate partitioning.

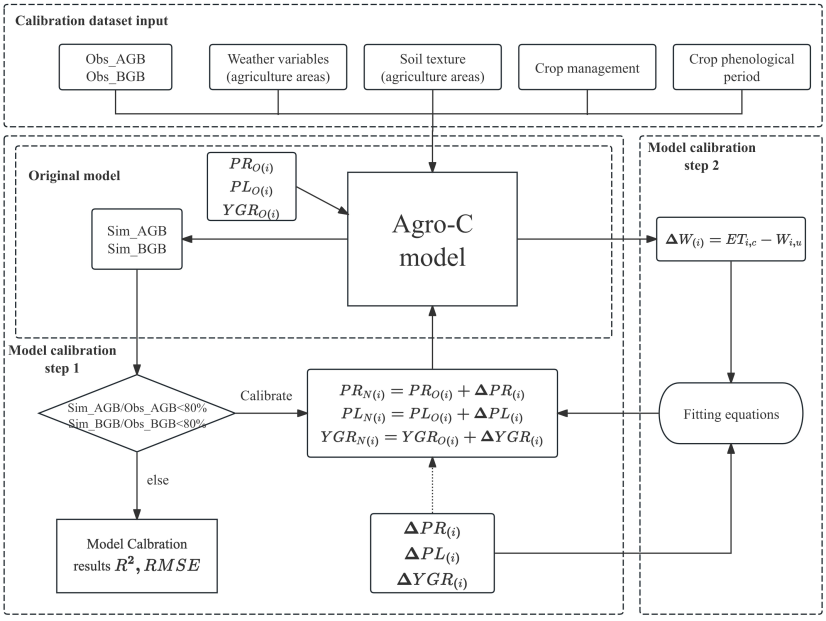

Fig. 1 Flowchart of Agro-C model parameter optimization

2.5 Data input and model evaluation

The input variables included: meteorological data (solar radiation, sunshine duration, daily maximum and minimum temperature, and precipitation); soil data (bulk density, sand and clay content, and total nitrogen content); phenological data (for wheat: emergence, heading, and maturity; for maize: emergence, tasseling, and maturity); and management practices (irrigation amount, fertilizer N application rate, and timing of application).

https://doi.org/10.5194/egusphere-2026-2303
Preprint. Discussion started: 27 May 2026

If irrigation amounts (W_{irr}) were recorded at the experimental sites for each crop growth stage, the values were directly input according to the recorded dates. If no specific irrigation amounts were available but the relative available soil water (RAW) during the growing season was recorded, the given RAW was used as the upper threshold to estimate irrigation. Irrigation was triggered when the model-simulated RAW dropped 10% below the site-defined threshold. The soil relative water content used in the model was calculated as follows:

$$\mathrm{RAW} = \frac{W_{(i)} - W_P}{W_{FC} - W_P} \times 100\% \quad (13)$$

where $W_{(i)}$ is the actual soil water content (v/v), W_P is the crop wilting point (v/v), and W_{FC} is the field capacity of the soil (v/v).

Irrigation amount was calculated as follows (Ge et al., 2012):

$$W_{irr} = (W_u - W_{(i)}) \times \rho \times h \times 0.1 \quad (14)$$

where W_u is the target upper limit of soil water content (v/v), ρ is the soil bulk density (g cm^{-3}), and h is the thickness of the soil layer considered (cm).

We used the coefficient of determination (R^2) and the root mean squared error (RMSE) as evaluation metrics to assess prediction accuracy, which are defined as follows:

$$R^2 = \frac{\sum_i (y_i - \widehat{y_i})^2}{\sum_i (y_i - \overline{y})^2} \quad (15)$$

$$RMSE = \sqrt{\frac{\sum_{i=1}^{n} (y_i - \widehat{y_i})^2}{n}} \quad (16)$$

where n is the number of test samples, y_i is the i observed value, $\overline{y}$ is the mean of all observed values, $\widehat{y_i}$ is the i simulate value.

3. Results

3.1 Optimization equations for photosynthate coefficients in response to soil moisture variation

https://doi.org/10.5194/egusphere-2026-2303
Preprint. Discussion started: 27 May 2026

3.1.1 Parameter optimization equations

To facilitate computation and maintain a balance between physiological resolution and numerical stability, the DVI was divided into 0.2 intervals, each representing a distinct growth stage relevant to crop development. To better capture the intra-stage variation of partitioning coefficients, DVI itself was also included as an independent variable in the equations (Tables 1 and 2). Consistent with the pre-optimized partitioning scheme of the model, we assumed that no leaf senescence occurred during the early vegetative stage (DVI < 0.6 for maize, DVI < 0.8 for wheat), with $YG_{R\_N} = 0$; and during the late reproductive stage (DVI > 1.4), assimilates were allocated only to grains, with the leaf partitioning coefficient set to zero. In the pre-optimized Agro-C model, assimilate allocation to roots (PR_N) was also assumed to cease once the crop entered the reproductive stage under sufficient water supply. However, our previous study (Xu et al., 2025) indicated that under water stress, assimilates may continue to be allocated to roots during the reproductive phase to facilitate water uptake and sustain growth. In addition, during the grain-filling to maturity stages (DVI=1.4–2.0), crops gradually enter physiological senescence, and root systems—particularly fine roots—undergo necrosis and shedding, leading to reduced accumulation of root dry matter. Therefore, we further refined the root partitioning scheme during the reproductive stage, building upon the pre-optimized framework.

https://doi.org/10.5194/egusphere-2026-2303
Preprint. Discussion started: 27 May 2026

Table 1 Wheat increments of Root (ΔPR) and Leaf (ΔPL) Allocation Coefficients, Yellow-to-Green Leaf Ratio (ΔYGR), and Water Balance Difference ($\Delta W_{(i)}$) Equation

$a + b*\Delta W_{(i)} + c*DVI + d*\Delta W_{(i)}^2 + e*\Delta W_{(i)}*DVI + f*DVI^2$

DVI		a	b	c	d	e	f	R^2	n	Range
	ΔPR	0.16	-0.29	-0.51	-0.13	1.47	1.40	0.06		[-0.1, 0.05]
(0.0, 0.2]	ΔPL	-0.56	3.32	6.83	1.72	-19.62	-17.95	0.13	438	[0.05, 0.15]
	ΔYGR				0.00					
	ΔPR	0.98	-0.62	-4.80	0.27	1.76	5.24	0.57	2150	[-0.2, 0.1]
(0.2, 0.4]	ΔPL	-8.73	-2.84	50.93	0.81	8.29	-72.50	0.20		[-0.1, 0.29]
	ΔYGR				0.00					
	ΔPR	0.20	0.12	-1.92	-0.02	-0.17	2.24	0.18		[-0.26, 0.1]
(0.4, 0.6]	ΔPL	-1.99	-1.43	7.92	0.01	2.32	-7.10	0.10	2567	[-0.16, 0.39]
	ΔYGR				0.00					
	ΔPR	0.21	-0.11	-1.16	0.02	0.10	1.08	0.47		[-0.1, 0.0]
(0.6, 0.8]	ΔPL	-2.35	-0.51	9.15	0.14	0.71	-8.33	0.16	655	[-0.15, 0.35]
	ΔYGR				0.00					
	ΔPR	-0.03	0.01	-0.49	0.00	-0.01	0.58	0.49		[-0.12, 0.15]
(0.8, 1.0]	ΔPL	-5.28	0.37	11.31	0.05	-0.64	-5.64	0.07	439	[-0.17, 0.46]
	ΔYGR	-0.57	-0.28	0.84	0.01	0.32	-0.72	0.05		[-0.43, 0.25]
	ΔPR	3.98	0.79	-7.82	0.00	-0.66	3.77	0.24		[-0.06, 0.06]
(1.0, 1.2]	ΔPL	-27.75	-1.10	54.01	0.07	0.95	-26.12	0.14	388	[0.0,0.36]
	ΔYGR	-21.40	-0.95	45.10	-0.06	0.92	-23.86	0.52		[-1.8, 0.4]
	ΔPR	-4.72	-0.01	7.46	-0.04	0.06	-2.97	0.14		[-0.1, 0.05]
(1.2, 1.4]	ΔPL	1.40	0.42	-1.82	-0.01	-0.30	0.59	0.17	305	[0.0, 0.2]
	ΔYGR	-8.49	6.08	12.73	-0.06	-4.76	-6.02	0.35		[-3.85, 0.68]
	ΔPR	-21.91	-1.31	28.98	-0.02	0.86	-9.60	0.12		[-0.06, 0.0]
(1.4, 1.6]	ΔPL				0.00				304	
	ΔYGR	-273.12	-5.71	379.64	-0.21	4.35	-133.41	0.14		[-5.0, 0.0]
	ΔPR	30.50	1.87	-38.69	0.00	-1.14	12.22	0.09		[-0.06, -0.03]
(1.6, 1.8]	ΔPL				0.00				288	
	ΔYGR	-510.13	1.23	612.27	0.69	-1.96	-184.75	0.11		[-6.4, 0.0]
	ΔPR	9.68	-9.64	-9.06	-0.26	5.31	2.04	0.16		[-0.06, 0.0]
(1.8, 2]	ΔPL				0.00				268	
	ΔYGR	-551.31	285.62	548.12	8.42	-157.41	-136.47	0.18		[-7.5, 0.0]

https://doi.org/10.5194/egusphere-2026-2303
Preprint. Discussion started: 27 May 2026

Table 2 Maize increments of Root (ΔPR) and Leaf (ΔPL) Allocation Coefficients, Yellow-to-Green Leaf Ratio (ΔYGR), and Water Balance Difference ($\Delta W_{(i)}$) Equation

$a + b*\Delta W_{(i)} + c*DVI + d*\Delta W_{(i)}^2 + e*\Delta W_{(i)}*DVI + f*DVI^2$

DVI		a	b	c	d	e	f	R^2	n	Range
(0.0, 0.2]	ΔPR	-0.15	-0.70	-0.09	0.53	3.76	-1.05	0.98	435	[-0.2, -0.1]
	ΔPL	0.19	0.56	0.07	-0.42	3.01	0.84	0.89		[0.19, 0.23]
	ΔYGR				0.00					
(0.2, 0.4]	ΔPR	0.60	-1.09	-6.22	0.34	3.84	11.35	0.89	383	[-0.25, -0.2]
	ΔPL	-3.09	4.20	24.02	-1.22	-14.89	-43.57	0.90		[0.05, 0.22]
	ΔYGR				0.00					
(0.4, 0.6]	ΔPR	5.47	-0.67	-26.86	0.00	1.52	31.64	0.92	389	[-0.25, 0.0]
	ΔPL	1.47	0.12	-5.41	0.07	-0.42	4.32	0.76		[0.0, 0.22]
	ΔYGR				0.00					
(0.6, 0.8]	ΔPR	-0.89	0.80	2.22	0.02	-1.11	-1.38	0.23	348	[-0.05, 0.05]
	ΔPL	-1.51	-0.09	3.44	0.00	0.13	-2.27	0.62		[-0.1, 0.11]
	ΔYGR	2.26	-2.84	-5.48	-0.09	3.97	3.36	0.24		[-0.03, 0.2]
(0.8, 1.0]	ΔPR				0.00				332	
	ΔPL	29.56	-0.43	-69.90	0.00	0.48	41.16	0.88		[-0.2, 0.11]
	ΔYGR	-65.17	0.40	151.25	0.00	-0.10	-87.51	0.43		[-0.07, 0.35]
(1.0, 1.2]	ΔPR	-6.08	1.11	9.59	-0.01	-1.01	-3.62	0.66	308	[0.0, 0.12]
	ΔPL	-118.10	2.26	206.59	0.07	-1.74	-90.19	0.42		[0.05, 0.45]
	ΔYGR	12.14	-0.05	-19.86	-0.05	0.03	7.99	0.42		[-0.14, 0.3]
(1.2, 1.4]	ΔPR	117.85	-1.74	-172.01	0.04	1.18	62.85	0.38	321	[0.0, 0.12]
	ΔPL	-213.00	3.34	311.30	-0.07	-2.28	-113.67	0.37		[0.0, 0.4]
	ΔYGR	120.52	-2.50	-175.84	0.05	1.72	64.04	0.40		[-0.48, 0.17]
(1.4, 1.6]	ΔPR	174.42	9.21	-247.65	0.13	-6.55	87.92	0.54	338	[-0.05, 0.12]
	ΔPL				0.00					
	ΔYGR	229.20	11.38	-326.10	0.16	-8.11	115.83	0.53		[-0.5, 0.0]
(1.6, 1.8]	ΔPR	259.85	3.67	-295.73	-0.03	-1.96	84.05	0.31	370	[-0.15, 0.0]
	ΔPL				0.00					
	ΔYGR	-838.08	6.24	1010.12	0.12	-4.20	-304.31	0.62		[-0.3, 0.15]
(1.8, 2]	ΔPR	0.80	3.13	-1.45	-0.20	-1.60	0.53	0.34	439	[-0.15, 0.0]
	ΔPL				0.00					
	ΔYGR	-246.13	16.95	263.13	0.90	-9.58	-70.43	0.38		[-0.6, 0.3]

https://doi.org/10.5194/egusphere-2026-2303
Preprint. Discussion started: 27 May 2026

3.1.2 Response of photosynthate allocation coefficients to soil moisture changes

We further analyzed the variation in assimilate allocation coefficients—PR , PL, and YGR—in response to soil moisture levels during key growth stages, including jointing stage, silking stage(maize), heading stage (wheat), and maturity (Fig. 2).

At the jointing stage (DVI = 0.4–0.6), maize PL significantly decreased with increasing soil moisture, while PR also showed a slight downward trend (Fig. 2(a)). In contrast, wheat PL was relatively insensitive to moisture changes, but under severe drought stress (RAW < 45%), wheat PR was significantly lower than under well-watered conditions (Fig. 2(d)). During the silking stage of maize (DVI = 1.0–1.2), both PL and YGR decreased with increasing soil moisture under moderate (RAW = 45–60%) and severe drought stress. However, under mild drought (RAW = 60–70%) to optimal moisture conditions, both PL and YGR increased with rising soil moisture. PR exhibited a non-linear response, increasing first and then decreasing as moisture increased (Fig. 2(b)). Similarly, at the wheat heading stage (DVI = 1.0–1.2), the trend of PR and YGR was comparable to that of maize, but wheat PL continuously decreased with increasing soil moisture, which is in contrast to maize (Fig. 2(e)).

At the maturity stage (DVI = 1.8–2.0), photosynthates were no longer allocated to leaves but instead to grains. Under drought stress, maize YGR increased significantly (Fig. 2(c)). Moreover, excess water (RAW > 85%) also led to higher YGR values than under optimal conditions (RAW = 70–85%). PR increased with rising soil moisture during this stage, as extreme drought caused premature root senescence and decay. Conversely, wheat PR and YGR decreased with increasing soil moisture during maturity (Fig. 2(f)). Notably, under severe drought conditions, wheat YGR was lower than under other moisture levels.

https://doi.org/10.5194/egusphere-2026-2303
Preprint. Discussion started: 27 May 2026

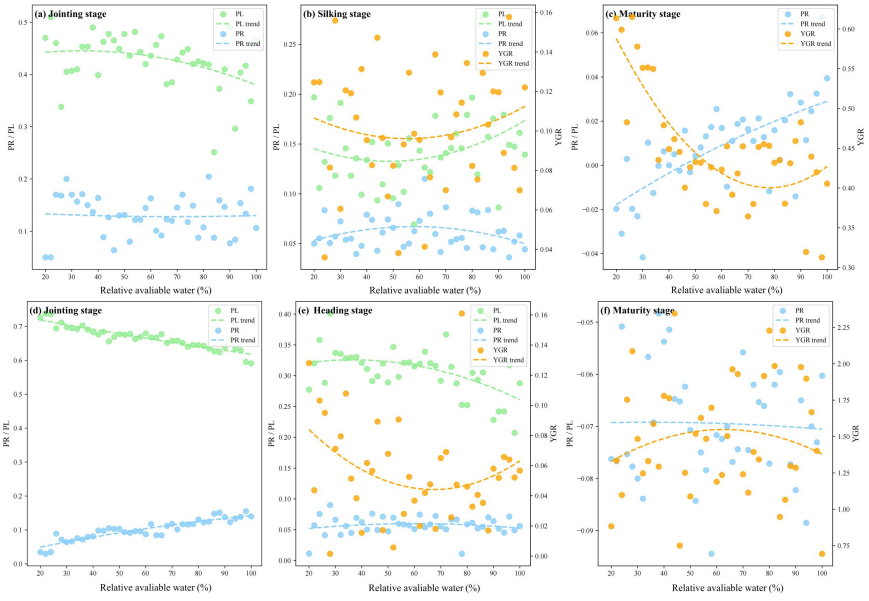

Fig. 2 Mean values of the leaf partitioning coefficient (PL), root partitioning coefficient (PR), and yellow-to-green leaf ratio (YGR) for maize and wheat at jointing, silking/heading, and maturity stages under different soil moisture conditions, as simulated by the optimized Agro-C model.

3.2 Model calibration and validation

3.2.1 Calibration results

We selected datasets that provided detailed records of aboveground biomass (AGB) and belowground biomass (BGB) at multiple crop growth stages, and which included experimental treatments under different levels of water stress, to serve as the calibration dataset. This allowed for more accurate simulation of assimilate partitioning across developmental stages.

Overall, the optimized Agro-C model showed higher accuracy in simulating AGB, with R^2 values exceeding 0.56 across all growth stages. In contrast, the simulation accuracy for BGB was relatively lower, with R^2 values ranging from 0.33 to 0.72 (Fig. 3). Notably, the optimized Agro-C model performed well in simulating AGB at maturity (Fig. 3(c)), with R^2 values of 0.89 for maize and 0.68 for wheat. Improved accuracy in simulating AGB at maturity contributes to more reliable estimation of crop productivity. The optimized Agro-C model showed better

https://doi.org/10.5194/egusphere-2026-2303
Preprint. Discussion started: 27 May 2026

328 performance in simulating wheat BGB (R^2 = 0.72) at the jointing stage compared to
329 maize (R^2 = 0.65). However, during the reproductive stage (silking to maturity for
330 maize; heading to maturity for wheat), simulation accuracy was higher for maize. For
331 maize, the optimized Agro-C model consistently achieved R^2 values above 0.63
332 across all growth stages, indicating a good performance.

333 Although the optimized Agro-C model showed relatively low R^2 values for
334 simulating wheat BGB at heading and maturity stages (0.33 and 0.44, respectively;
335 Fig. 3(e-f)), this was primarily attributed to physiological root senescence during late
336 reproductive stages, leading to lower root biomass per unit area. Under such
337 conditions, the absolute values of BGB were small, and even slight deviations
338 between simulated and observed values could substantially reduce R^2. Nevertheless,
339 the RMSE for wheat BGB at heading and maturity were 8.45 and 8.23 gC m^{-2},
340 respectively, indicating relatively small deviations. Therefore, we consider the
341 optimized Agro-C model to be reasonably reliable and practically applicable for
342 simulating BGB for wheat during the later reproductive stages.

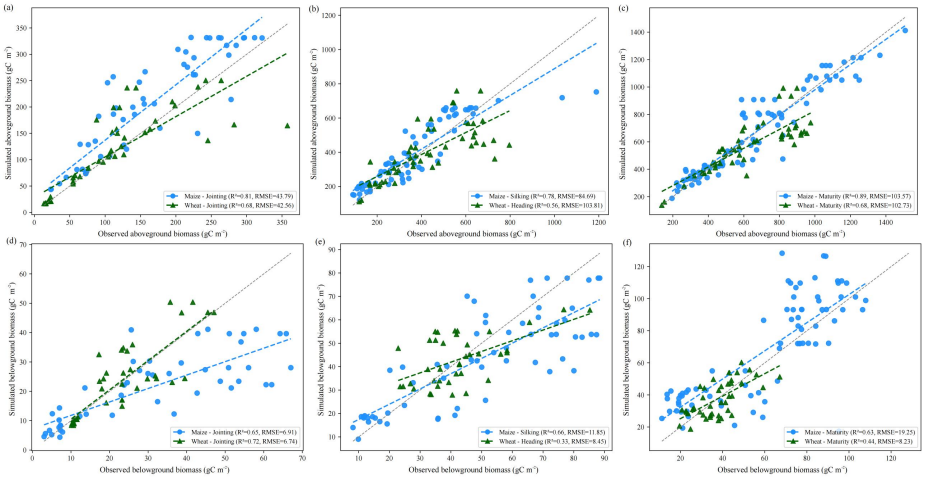

343

344 Fig. 3 Calibration results of the Agro-C model for aboveground biomass (AGB) and belowground
345 biomass (BGB) of maize and wheat at the jointing, heading/grain-filling, and maturity stages.
346 (a)–(c) show AGB calibration results; (d)–(f) show BGB calibration results. Blue circles represent
347 maize, and green triangles represent wheat.

https://doi.org/10.5194/egusphere-2026-2303
Preprint. Discussion started: 27 May 2026

3.2.2 Validation results

Due to limited availability of experimental data, the criteria for selecting the validation dataset were less stringent than those applied to the calibration dataset. Therefore, datasets that included detailed records of water use during the crop growth period (regardless of whether water stress treatments were applied) and biomass data for one or more growth stages were included in the validation dataset.

Compared with the pre-optimized Agro-C model, the optimized Agro-C model showed substantial improvements in simulating assimilate production for both maize and wheat (Fig. 4). For maize, the simulation accuracy for AGB improved from R^2 = 0.70 and RMSE = 153.15 gC m^{-2} to R^2 = 0.95 and RMSE = 66.03 gC m^{-2}. Similarly, the BGB simulation improved from R^2 = 0.49 and RMSE = 20.55 gC m^{-2} to R^2 = 0.61 and RMSE = 11.18 gC m^{-2}. Likewise, for wheat, the optimized Agro-C model significantly improved the simulation accuracy for both AGB and BGB, achieving R^2 values of 0.74 (RMSE = 60.26 gC m^{-2}) for AGB and 0.48 (RMSE = 19.43 gC m^{-2}) for BGB, compared to the pre-optimized Agro-C model, which simulate AGB and BGB much lower R^2 values of 0.31 and 0.42, respectively. The validation dataset comprised several water-stress treatments, the pre-optimized Agro-C model simulation accuracy declined under these conditions due to the absence of water stress-responsive allocation parameters in the pre-optimized structure.

Similar to the calibration results, the optimized Agro-C model exhibited significantly higher accuracy in simulating AGB than BGB for the validation dataset. However, after parameter optimization, the average differences between simulated and observed BGB for maize and wheat were only 5.19 and -2.52 gC m^{-2}, respectively (Fig. S2), indicating relatively small deviations. In addition, compared to pre-optimized Agro-C model, the optimized Agro-C model exhibited consistently smaller deviations from the observed values (Fig. S2), suggesting a relatively reliable parameter calibration scheme.

https://doi.org/10.5194/egusphere-2026-2303
Preprint. Discussion started: 27 May 2026

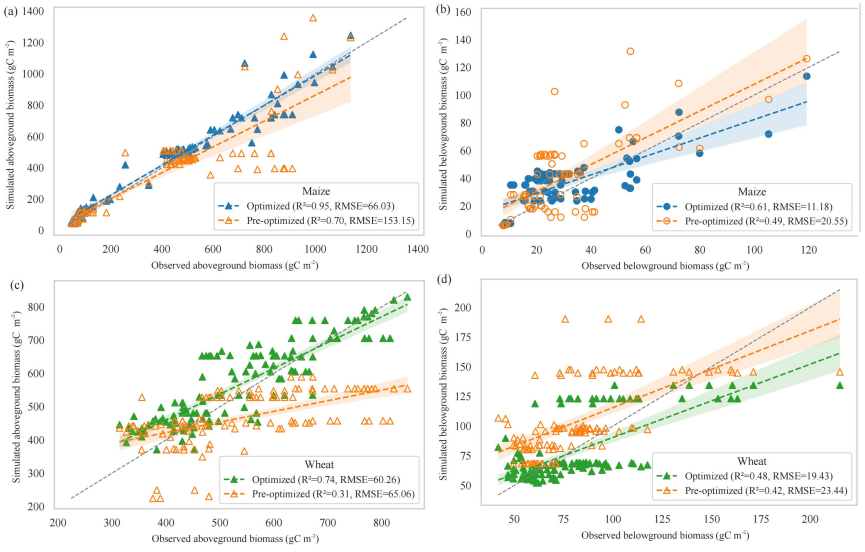

Fig. 4 Validation results of the pre-optimized and optimized Agro-C model for simulating aboveground biomass (AGB) and belowground biomass (BGB) of maize and wheat. (a) and (b) show the validation results for maize AGB and BGB, respectively; (c) and (d) show the validation results for wheat AGB and BGB, respectively. Blue circles and green triangles represent the simulation results from the optimized model, while orange hollow circles and triangles represent the simulation results from the pre-optimized Agro-C model for maize and wheat, respectively.

3.3 Simulating photosynthetic biomass under different RAW

Based on the observed patterns, four distinct soil moisture regimes were defined: severe drought (RAW < 45%), mild-to-moderate drought (RAW = 45–70%), optimal moisture (RAW = 70–85%), and excessive moisture (RAW > 85%). Simulations of maize and wheat AGB and BGB were conducted under each condition (Figs. 5-8).

Since the pre-optimized Agro-C model did not adequately account for crop growth under water-deficit conditions, its performance in simulating photosynthate production under water stress (RAW < 70%) was unsatisfactory, resulting in low R^2 values and relatively high RMSE. However, under optimal moisture conditions, the pre-optimized model performed well, particularly in simulating AGB, demonstrating its high applicability in well-watered environments. The optimized Agro-C model showed marked improvements across all moisture regimes. The R^2 of AGB simulation for maize ranged from 0.77 to 0.95, and for wheat from 0.80 to 0.89,

https://doi.org/10.5194/egusphere-2026-2303
Preprint. Discussion started: 27 May 2026

397 respectively (Figs. 5 and 7), demonstrating that the optimized Agro-C model
398 performed well in simulating AGB across different soil moisture conditions. This
399 strong performance enhances its applicability for crop productivity estimation and
400 quantification of straw return to the field. For wheat BGB, the optimized Agro-C
401 model achieved R^2 values of 0.77–0.83 (Fig. 8), greatly improving the accuracy
402 compared to the pre-optimized Agro-C model (R^2 in 0.52–0.78), which previously
403 exhibited large errors in simulating wheat BGB. Under varying soil moisture
404 conditions, the optimized Agro-C model achieved R^2 values of 0.62 to 0.74 for
405 simulating maize BGB, consistently outperforming pre-optimized Agro-C model.
406 Notably, the accuracy of the optimized Agro-C model was significantly improved
407 under severe and mild-to-moderate drought, highlighting its enhanced responsiveness
408 to water stress.

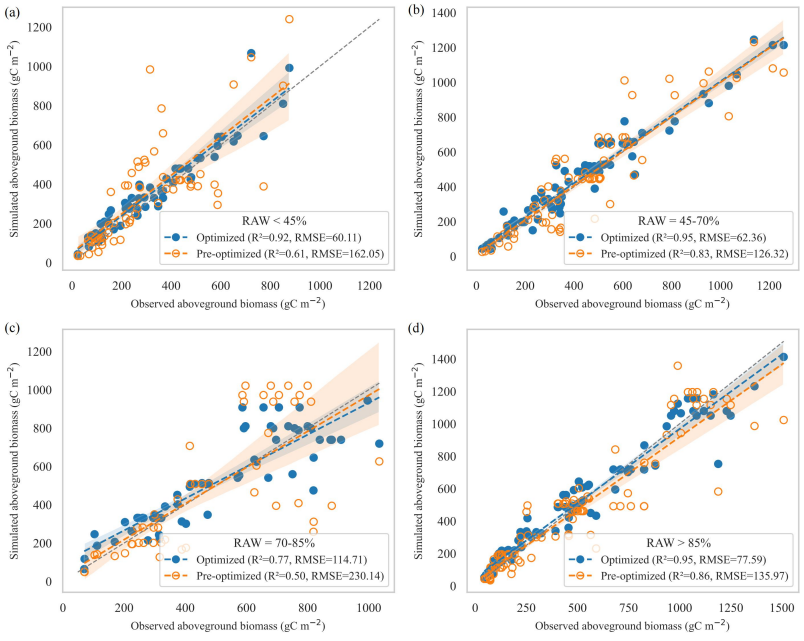

409

410 Fig. 5 Simulated aboveground biomass (AGB) of maize under different relative available
411 soil water (RAW) conditions using the pre-optimized Agro-C model and the optimized
412 Agro-C model. Blue circles represent simulation results from the optimized Agro-C model,
413 and orange circles represent those from the pre-optimized Agro-C model.

https://doi.org/10.5194/egusphere-2026-2303
Preprint. Discussion started: 27 May 2026

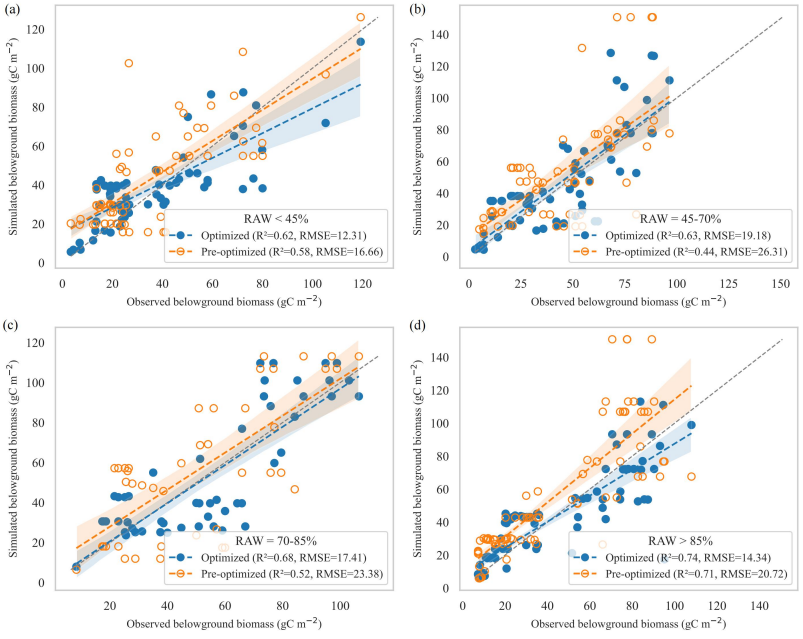

414

415 Fig. 6 Simulated belowground biomass (BGB) of maize under different relative available
416 soil water (RAW) conditions using the pre-optimized Agro-C model and the optimized
417 Agro-C model. Blue circles represent simulation results from the optimized Agro-C model,
418 and orange circles represent those from the pre-optimized Agro-C model.

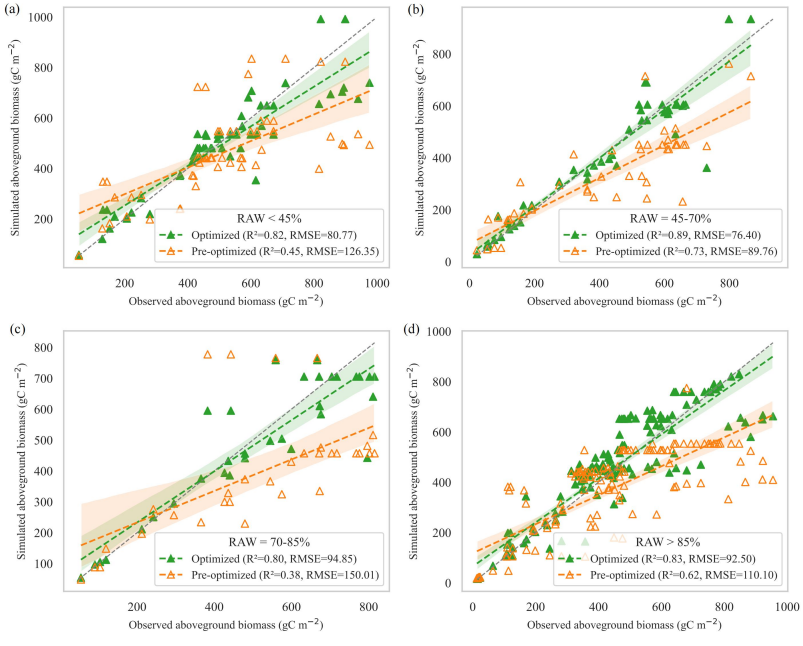

419

https://doi.org/10.5194/egusphere-2026-2303
Preprint. Discussion started: 27 May 2026

Fig. 7 Simulated aboveground biomass (AGB) of wheat under different relative available soil water (RAW) conditions using the pre-optimized Agro-C model and the optimized Agro-C model. Green triangles represent simulation results from the optimized Agro-C model, and orange triangles represent those from the pre-optimized Agro-C model.

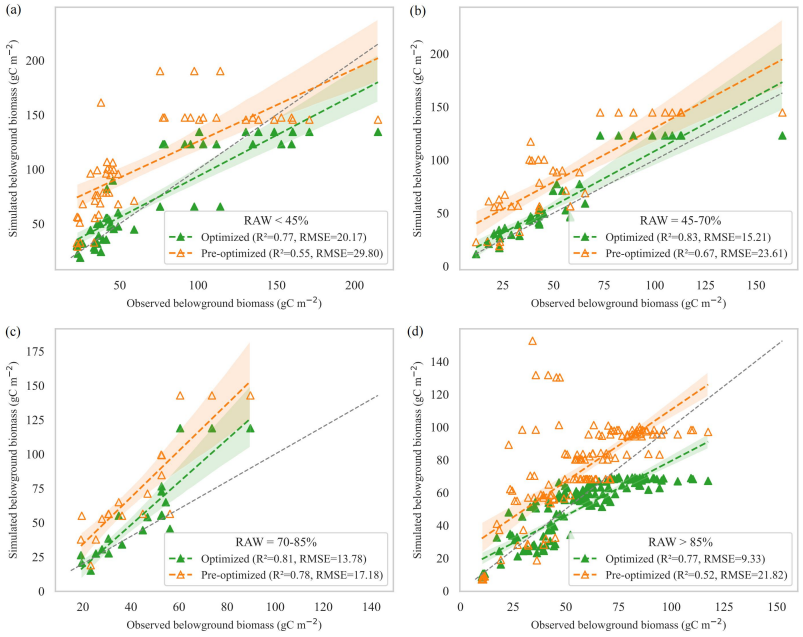

Fig. 8 Simulated belowground biomass (BGB) of wheat under different relative available soil water (RAW) conditions using the pre-optimized Agro-C model and the optimized Agro-C model. Green triangles represent simulation results from the optimized Agro-C model, and orange triangles represent those from the pre-optimized Agro-C model.

4. Discussion

4.1 Model performance evaluation

By incorporating dynamic response functions of photosynthate allocation coefficients to water stress and developmental stage, the optimized Agro-C model achieved significantly improved simulation accuracy across both crops and growth phases. Overall, the model exhibited higher accuracy for simulating AGB than BGB, a trend consistently observed in both the calibration and validation datasets (Fig. 3, Fig. 4). This likely reflects more abundant observations and better mechanistic understanding for aboveground processes, improving predictability (Asseng et al.,

https://doi.org/10.5194/egusphere-2026-2303
Preprint. Discussion started: 27 May 2026

2013; Li et al., 2015).

Although the optimized Agro-C model better simulated wheat AGB and BGB during the jointing stage, its accuracy was surpassed by maize simulations during the reproductive phase. This contrast can be attributed to the distinct allocation strategies between the two crops during the reproductive transition. For wheat, photosynthate allocation during the jointing stage is relatively straightforward, focusing primarily on leaf expansion and root development—processes that are easier to capture through modeling. However, during the reproductive phase, grain filling in wheat relies heavily on the remobilization of stem-reserved assimilates (Bertheloot et al., 2008; Effah et al., 2022), while the root system undergoes rapid senescence (Wang et al., 2014), complicating model representation. The model's simplified structure does not fully capture belowground complexities, resulting in low R^2 values (0.33-0.44) during heading and maturity. However, due to small BGB magnitudes, even modest deviations result in relatively low RMSE values (8.45 and 8.23 gC m^{-2}), indicating reasonable model performance at the magnitude level. In contrast, as a C4 crop, maize relies more directly on continuous leaf photosynthesis for grain formation (Boyer & Westgate, 2004). Water stress markedly suppresses leaf expansion and photosynthetic activity, but leaf area index can recover following rehydration, enhancing aboveground dry matter accumulation (Ma et al., 2025). Therefore, the dynamic adjustment of water and leaf allocation functions enhances model performance for simulating maize biomass during the reproductive stage.

The inclusion of multiple water stress trials in the validation dataset, pre-optimized Agro-C model showed unsatisfactory performance (low R^2, high RMSE) due to lacking water stress response, while the optimized Agro-C model better captured photosynthetic biomass allocation under stress (Figs. 4 and S2). This further demonstrates that incorporating water-sensitive parameters into allocation functions is a critical strategy for enhancing the drought responsiveness of crop models (Monteleone et al., 2023; Hammer et al., 2010). Following parameter optimization, the simulation accuracy of Agro-C was significantly improved across all

https://doi.org/10.5194/egusphere-2026-2303
Preprint. Discussion started: 27 May 2026

water regimes, with the most notable enhancement observed in the simulation of belowground biomass. This effectively corrected the bias of pre-optimized Agro-C model in representing root dynamics. Given that BGB is a major contributor to SOC, improved simulation of root biomass reduces uncertainties in SOC modeling, thereby enabling more accurate assessment of SOC stocks.

Nevertheless, limitations remain in the current version of the model. The overall accuracy for simulating BGB is lower than that for AGB, suggesting that the dynamic processes governing root growth and senescence are not yet fully captured. Previous studies have highlighted that root architecture (e.g., deep vs. shallow rooting types), interactions among water availability, nitrogen input, and temperature, as well as carbon remobilization mechanisms, can all influence model performance (Lynch et al., 2014; Calleja-Cabrera et al., 2022; Li et al., 2025). These processes should be incorporated into future model development to enhance representation of belowground dynamics.

4.2 Effect of soil water on photosynthate allocation across crop growth

The response of photosynthate allocation to water stress exhibits strong stage dependence and crop specificity. Using continuous DVI-based allocation functions (Tables 1 and 2), it is evident that during the vegetative stage, both maize and wheat adopt a “root-priority” strategy to enhance water uptake under drought stress, as reflected by a significant increase in the PR and a concurrent decrease in the PL (Fig. 2(a) and (d); Çakir, 2004). As crops transition into the reproductive phase, maize at silking and wheat at heading display heightened sensitivity of partitioning coefficients to soil moisture. Under moderate to severe drought conditions (RAW < 60%), both maize and wheat exhibit decreasing trends in PL and YGR with increasing soil moisture (Fig. 2(b) and (e)), likely due to impaired plant capacity to maintain photosynthetic area and delay leaf senescence under water-limited conditions (Vadez et al., 2024). Interestingly, under mild drought to optimal water conditions (RAW = 60–85%), maize exhibits increasing PL and YGR with increasing moisture, indicating that appropriate irrigation during this stage effectively alleviates water stress and

https://doi.org/10.5194/egusphere-2026-2303
Preprint. Discussion started: 27 May 2026

promotes greater allocation of photosynthates to foliage (Ma et al., 2025).

Notably, maize and wheat also exhibit divergent biomass allocation patterns when exposed to water stress at the same developmental stage. During the reproductive transition phase, maize exhibited a significant increase in PL under optimal water conditions, accompanied by a peak in leaf area index (LAI), which helps maintain leaf functionality and ensures successful pollination and kernel formation (Ma et al., 2025). In contrast, wheat showed a continuous decline in PL, suggesting that photosynthates were increasingly diverted to the developing spike during anthesis stage, indicating a reduced dependence on leaf investment (Farooq et al., 2014). This divergence underscores an evolutionary trade-off between C4 and C3 crops in carbon-use efficiency. Under water stress, maize prioritizes the protection of leaf function, whereas wheat ensures grain filling through strategic assimilate redistribution (Borrás et al., 2004; Smith et al., 2018). At maturity, maize roots senesce prematurely under drought, leading to a decline in PR, while under optimal or excessive moisture conditions, PR increases (Fig. 2(c)). In contrast, wheat exhibits a consistent decline in both PR and YGR with increasing soil moisture (Fig. 2(f)), confirming that root senescence in late grain filling enables greater carbon allocation to kernels, ultimately enhancing yield potential.

In addition, excess water also significantly affects the partitioning of photosynthates. During maize maturity, YGR under conditions of excessive moisture (RAW > 85%) was higher than under optimal water supply, suggesting that overwatering may induce premature leaf senescence and accelerate assimilate translocation to the grain. Excessive soil moisture reduces root aeration and increases respiratory losses, thereby weakening root activity (Shao et al., 2013; Herzog et al., 2015). Thus, excessive water supply can also disrupt the optimal partitioning of photosynthates, ultimately compromising yield formation. For maize, it is crucial to avoid both drought stress and over-irrigation during silking and maturity stages to maintain leaf function and root vitality. For wheat, particular attention should be paid to water supply during the jointing to heading stages to ensure proper spike

https://doi.org/10.5194/egusphere-2026-2303
Preprint. Discussion started: 27 May 2026

differentiation and grain development.

4.3 Representation of water stress responses in the Agro-C model

Existing crop models adopt various approaches to represent water stress. For instance, the DSSAT model constructs stress coefficients based on the ratio of soil water supply to demand, applying them to processes such as photosynthesis, transpiration, leaf area development, and biomass accumulation (Jones et al., 2003; He et al., 2013). While effective in reflecting drought-induced reductions in photosynthetic and transpiration rates, DSSAT often employs fixed or stage-specific allocation schemes, lacking the capacity to dynamically redistribute assimilates among plant organs. The APSIM model uses stress factors to simulate water stress effects on root growth, leaf area expansion, and photosynthesis, with a modular and transparent structure enabling its application across diverse cropping systems (Pasley et al., 2020; Githui et al., 2022; Monteleone et al., 2023). However, APSIM relies on empirical functions and does not explicitly model the dynamic carbon allocation among roots, leaves, and grains, limiting its explanatory power at the organ scale. The AquaCrop model uses threshold-based functions to simulate water stress effects on canopy expansion, stomatal conductance, leaf senescence, and harvest index, performing well for yield and water-use efficiency under drought, though it oversimplifies root biomass by relying on RSR adjustments and lacks mechanisms for root senescence and dynamic carbon allocation (Zhou et al., 2024; Fallah et al., 2025).

Compared with the aforementioned models, the optimized Agro-C model developed in this study improves the representation of photosynthate allocation under water stress by more explicitly reflecting underlying physiological regulation. By linking partitioning coefficients (PL and PR) and YGR to both soil moisture and DVI, the model explicitly captures organ-level carbon allocation under water stress. This improves its ability to represent key physiological responses such as root-priority allocation and premature leaf senescence, enhancing simulation accuracy across moisture conditions. Moreover, the optimized Agro-C model captures the water-dependent variability in carbon partitioning during key growth stages

https://doi.org/10.5194/egusphere-2026-2303
Preprint. Discussion started: 27 May 2026

overcoming the limitations of conventional models that rely on fixed rules or lack dynamic regulation across stages. Finally, the parameter calibration is based on observed AGB and BGB data, enabling the model to not only simulate yield variations, but also provide mechanistic representation insights into organ-level allocation dynamics, thereby improving its physiological interpretability and robustness.

However, the current scheme still simplifies root processes by adjusting root allocation coefficients solely based on water status, without accounting for key parameters such as root architecture and turnover rate—factors that are particularly critical under extreme moisture conditions (Lynch et al., 2014). Overall, the optimized Agro-C model proves capable of capturing carbon allocation under diverse water regimes, suggesting strong applicability. In the future, the proposed framework can potentially be integrated into land surface and Earth system models to improve the representation of carbon–water coupling under future climate scenarios.

5. Conclusion

This study incorporated water stress effects into crop carbon allocation by linking the root and leaf partitioning coefficients (PR and PL) and the yellow-to-green leaf ratio (YGR) to soil moisture and DVI, thereby optimizing the Agro-C model. The optimized Agro-C model addresses limitations of fixed partitioning rules by capturing stage-sensitive responses and dynamic shifts in allocation under drought and over-irrigation. Compared with the pre-optimized Agro-C model, the optimized Agro-C model demonstrated a substantial improvement in simulation accuracy, achieving R^2 values of 0.74-0.95 for AGB and 0.48 - 0.61 for BGB in validation datasets. Moreover, the optimized Agro-C model effectively captured biomass dynamics across a wide range of soil moisture conditions—from drought to excessive moisture—achieving R^2 values of 0.77-0.95 for AGB and 0.62-0.83 for BGB in maize and wheat, thereby demonstrating improved robustness and physiological fidelity. Nonetheless, the representation of root system architecture and turnover remains simplified, highlighting the need for further mechanistic refinement. Overall, the

https://doi.org/10.5194/egusphere-2026-2303
Preprint. Discussion started: 27 May 2026

model presents a robust tool for simulating drought-induced carbon allocation strategies and can be applied in broader climate–agriculture interactions to inform sustainable water and carbon management strategies.

Author contributions

WZ, QZ and YY elaborated the algorithmic concept; WX implemented the codes, conducted the numerical experiments, visualized the results, and prepared the manuscript. All authors reviewed and edited the manuscript.

Competing interests

The authors declare that they have no known competing financial interests or personal relationships that could have appeared to influence the work reported in this paper.

Disclaimer. Publisher's note:

Copernicus Publications remains neutral with regard to jurisdictional claims made in the text, published maps, institutional affiliations, or any other geographical representation in this paper. While Copernicus Publications makes every effort to include appropriate place names, the final responsibility lies with the authors.

Code and data availability

The code that support the findings of this study are openly available in Zenodo at Xu et al. (2026; https://doi.org/10.5281/zenodo.19970992), reference number 19970992. All data used in this study are publicly available. Meteorological data for the crop growing period were obtained from *ERA5* (https://cds.climate.copernicus.eu/). The calibration data of the model are sourced from Duan (2020); Feng et al. (1997); Feng (2014); Ge et al. (2005); Ge et al. (2012); Gheysari et al. (2017); Jiang (2019); Li et al. (2010); Lu et al.(2020); Wang (2011); Wang et al. (2014); Wang (2014); Zhang (2023). The validation data of the model are sourced from Allard et al. (2013); Cai et al. (2017); Chen et al. (2021); Fang et al. (2017); Liu et al. (2017); Núñez et al. (2022); Pouri et al. (2019); Xu et al. (2020); Zhao et al. (2018); Zou et al. (2021).

https://doi.org/10.5194/egusphere-2026-2303
Preprint. Discussion started: 27 May 2026

Acknowledgments

This study was financially supported by the National Natural Science Foundation of China (42171064), the National Key R&D Program of China (2022YFD1901604) and the Key Research and Development Program of Yunnan Province (202303AC100009).

https://doi.org/10.5194/egusphere-2026-2303
Preprint. Discussion started: 27 May 2026

References

Ahuja, L., Ma, L., Timlin, D., Stockle, C., and Boote, K. J.: Current Water Deficit Stress Simulations in Selected Agricultural System Models, Response of Crops to Limited Water: Understanding and Modeling Water Stress Effects on Plant Growth Processes, https://doi.org/10.2134/advagricsystmodel1.c1, 2008.

Allard, V., Martre, P., and Le Gouis, J.: Genetic variability in biomass allocation to roots in wheat is mainly related to crop tillering dynamics and nitrogen status, European Journal of Agronomy, 46, 68–76, https://doi.org/10.1016/j.eja.2012.12.004, 2013.

Allen, R. G., Pereira, L. S., Smith, M., Raes, D., and Wright, J. L.: FAO-56 Dual Crop Coefficient Method for Estimating Evaporation from Soil and Application Extensions, J. Irrig. Drain Eng., 131, 2–13, https://doi.org/10.1061/(ASCE)0733-9437(2005)131:1(2), 2005.

Allen, R. G., Pruitt, W. O., Wright, J. L., Howell, T. A., Ventura, F., Snyder, R., Itenfisu, D., Steduto, P., Berengena, J., Yrisarry, J. B., Smith, M., Pereira, L. S., Raes, D., Perrier, A., Alves, I., Walter, I., and Elliott, R.: A recommendation on standardized surface resistance for hourly calculation of reference ETo by the FAO56 Penman-Monteith method, Agricultural Water Management, 81, 1–22, https://doi.org/10.1016/j.agwat.2005.03.007, 2006.

Asseng, S., Ewert, F., Rosenzweig, C., Jones, J. W., Hatfield, J. L., Ruane, A. C., Boote, K. J., Thorburn, P. J., Rötter, R. P., Cammarano, D., Brisson, N., Basso, B., Martre, P., Aggarwal, P. K., Angulo, C., Bertuzzi, P., Biernath, C., Challinor, A. J., Doltra, J., Gayler, S., Goldberg, R., Grant, R., Heng, L., Hooker, J., Hunt, L. A., Ingwersen, J., Izaurralde, R. C., Kersebaum, K. C., Müller, C., Naresh Kumar, S., Nendel, C., O'Leary, G., Olesen, J. E., Osborne, T. M., Palosuo, T., Priesack, E., Ripoche, D., Semenov, M. A., Shcherbak, I., Steduto, P., Stöckle, C., Stratonovitch, P., Streck, T., Supit, I., Tao, F., Travasso, M., Waha, K., Wallach, D., White, J. W., Williams, J. R., and Wolf, J.: Uncertainty in simulating wheat yields under climate change, Nature Clim Change, 3, 827–832, https://doi.org/10.1038/nclimate1916, 2013.

Bernacchi, C. J. and VanLoocke, A.: Terrestrial Ecosystems in a Changing Environment: A Dominant Role for Water, Annu. Rev. Plant Biol., 66, 599–622, https://doi.org/10.1146/annurev-arplant-043014-114834, 2015.

Bertheloot, J., Martre, P., and Andrieu, B.: Dynamics of Light and Nitrogen Distribution during Grain Filling within Wheat Canopy, Plant Physiol, 148, 1707–1720, https://doi.org/10.1104/pp.108.124156, 2008.

Boretti, A. and Rosa, L.: Reassessing the projections of the World Water Development Report, npj Clean Water, 2, 15, https://doi.org/10.1038/s41545-019-0039-9, 2019.

Borrás, L., Slafer, G. A., and Otegui, M. E.: Seed dry weight response to source–sink manipulations in wheat, maize and soybean: a quantitative reappraisal, Field Crops Research, 86, 131–146, https://doi.org/10.1016/j.fcr.2003.08.002, 2004.

Boyer, J. S.: Grain yields with limited water, Journal of Experimental Botany, 55, 2385–2394, https://doi.org/10.1093/jxb/erh219, 2004.

Cai, Q., Zhang, Y., Sun, Z., Zheng, J., Bai, W., Zhang, Y., Liu, Y., Feng, L., Feng, C., Zhang, Z.,

https://doi.org/10.5194/egusphere-2026-2303
Preprint. Discussion started: 27 May 2026

Yang, N., Evers, J. B., and Zhang, L.: Morphological plasticity of root growth under mild water stress increases water use efficiency without reducing yield in maize, Biogeosciences, 14, 3851–3858, https://doi.org/10.5194/bg-14-3851-2017, 2017.

Cai, G., Ahmed, M. A., Abdalla, M., and Carminati, A.: Root hydraulic phenotypes impacting water uptake in drying soils, Plant, Cell & Environment, 45, 650–663, https://doi.org/10.1111/pce.14259, 2022.

Çakir, R.: Effect of water stress at different development stages on vegetative and reproductive growth of corn, Field Crops Research, 89, 1–16, https://doi.org/10.1016/j.fcr.2004.01.005, 2004.

Calleja-Cabrera, J., Boter, M., Oñate-Sánchez, L., and Pernas, M.: Root Growth Adaptation to Climate Change in Crops, Front. Plant Sci., 11, https://doi.org/10.3389/fpls.2020.00544, 2020.

Chen, R., Xiong, X., and Cheng, W.: Root characteristics of spring wheat under drip irrigation and their relationship with aboveground biomass and yield, Sci Rep, 11, 4913, https://doi.org/10.1038/s41598-021-84208-7, 2021.

Chen, Z., Niu, Y., Zhao, R., Han, C., Han, H., and Luo, H.: The combination of limited irrigation and high plant density optimizes canopy structure and improves the water use efficiency of cotton, Agricultural Water Management, 218, 139–148, https://doi.org/10.1016/j.agwat.2019.03.037, 2019.

Cook, B. I., Smerdon, J. E., Seager, R., and Coats, S.: Global warming and 21st century drying, Clim Dyn, 43, 2607–2627, https://doi.org/10.1007/s00382-014-2075-y, 2014.

Dai, A.: Increasing drought under global warming in observations and models, Nature Clim Change, 3, 52–58, https://doi.org/10.1038/nclimate1633, 2013.

Duan, W.: Dynamic Response of Root-shoot Growth of Summer Maize to Soil Moisture under Deficit Irrigation, Northwest A&F University in Partial Fulfillment of the Requirements, 2022.

van Diepen, C. a., Wolf, J., van Keulen, H., and Rappoldt, C.: WOFOST: a simulation model of crop production, Soil Use and Management, 5, 16–24, https://doi.org/10.1111/j.1475-2743.1989.tb00755.x, 1989.

Dodd, I. C., Egea, G., Watts, C. W., and Whalley, W. R.: Root water potential integrates discrete soil physical properties to influence ABA signalling during partial rootzone drying, Journal of Experimental Botany, 61, 3543–3551, https://doi.org/10.1093/jxb/erq195, 2010.

Effah, Z., Li, L., Xie, J., Karikari, B., Wang, J., Zeng, M., Wang, L., Boamah, S., and Padma Shanthi, J.: Post-anthesis Relationships Between Nitrogen Isotope Discrimination and Yield of Spring Wheat Under Different Nitrogen Levels, Front. Plant Sci., 13, https://doi.org/10.3389/fpls.2022.859655, 2022.

Fallah, M., Rasulov, A., Ekambaram, Y., Khudayberganov, K., Devi Kosuru, S. n. v. j., and Ghate, A. D.: Simulating Plant Growth Under Water Stress Using the AquaCrop Model, Natural and Engineering Sciences, 10, 447–458, https://doi.org/10.28978/nesciences.1763853, 2025.

https://doi.org/10.5194/egusphere-2026-2303
Preprint. Discussion started: 27 May 2026

694 Fang, Y., Du, Y., Wang, J., Wu, A., Qiao, S., Xu, B., Zhang, S., Siddique, K.H.M., Chen, Y.:
695 Moderate Drought Stress Affected Root Growth and Grain Yield in Old, Modern and Newly
696 Released Cultivars of Winter Wheat, Front. Plant Sci. 8, 672,
697 https://doi.org/10.3389/fpls.2017.00672, 2017.

698 Farooq, M., Wahid, A., Kobayashi, N., Fujita, D., and Basra, S. M. A.: Plant drought stress:
699 effects, mechanisms and management, Agron. Sustain. Dev., 29, 185–212,
700 https://doi.org/10.1051/agro:2008021, 2009.

701 Farooq, M., Hussain, M., and Siddique, K. H. M.: Drought Stress in Wheat during Flowering and
702 Grain-filling Periods, Critical Reviews in Plant Sciences, 33, 331–349,
703 https://doi.org/10.1080/07352689.2014.875291, 2014.

704 Feng, G., Luo, Y.: Simulation on Functional Equilibrium of Winter Wheat Root and Shoot under
705 Different Soil Water Regimes, Acta Ecologica Sinica 19, 1, 1999.

706 Feng, H., Tan, X., Bi, Jian.: Study on the Root Distribution and Root Characteristics of Winter
707 Wheat under Different Soil and Water Conditions, Journal of Anhui Agri. Sci. 2013, 41(35) :
708 13465 - 13467,13471, 2013.

709 Field, C. B., Randerson, J. T., and Malmström, C. M.: Global net primary production: Combining
710 ecology and remote sensing, Remote Sensing of Environment, 51, 74–88,
711 https://doi.org/10.1016/0034-4257(94)00066-V, 1995.

712 Ge, T., Sui, F., Li, J., Lv, Y., Zhou, G.: Effects of Drought on Growth of Root and Shoot of
713 Summer Maize, Chinese Agricultural Science Bulletin 21, 1, 2005.

714 Ge, T., Sui, F., Bai, L., Tong, C., and Sun, N.: Effects of water stress on growth, biomass
715 partitioning, and water-use efficiency in summer maize (Zea mays L.) throughout the growth
716 cycle, Acta Physiol Plant, 34, 1043–1053, https://doi.org/10.1007/s11738-011-0901-y, 2012.

717 Gheysari, M., Sadeghi, S.-H., Loescher, H. W., Amiri, S., Zareian, M. J., Majidi, M. M., Asgarinia,
718 P., and Payero, J. O.: Comparison of deficit irrigation management strategies on root, plant
719 growth and biomass productivity of silage maize, Agricultural Water Management, 182,
720 126–138, https://doi.org/10.1016/j.agwat.2016.12.014, 2017.

721 Githui, F., Beverly, C., Aiad, M., McCaskill, M., Liu, K., and Harrison, M. T.: Modelling
722 Waterlogging Impacts on Crop Growth: A Review of Aeration Stress Definition in Crop
723 Models and Sensitivity Analysis of APSIM, International Journal of Plant Biology, 13,
724 180–200, https://doi.org/10.3390/ijpb13030017, 2022.

725 Gupta, A., Rico-Medina, A., and Caño-Delgado, A. I.: The physiology of plant responses to
726 drought, Science, 368, 266–269, https://doi.org/10.1126/science.aaz7614, 2020.

727 Hafner, B. D., Hesse, B. D., Bauerle, T. L., and Grams, T. E. E.: Water potential gradient, root
728 conduit size and root xylem hydraulic conductivity determine the extent of hydraulic
729 redistribution in temperate trees, Functional Ecology, 34, 561–574,
730 https://doi.org/10.1111/1365-2435.13508, 2020.

731 Hammer, G. L., Van Oosterom, E., McLean, G., Chapman, S. C., Broad, I., Harland, P., and
732 Muchow, R. C.: Adapting APSIM to model the physiology and genetics of complex adaptive
733 traits in field crops, Journal of Experimental Botany, 61, 2185–2202,

https://doi.org/10.5194/egusphere-2026-2303
Preprint. Discussion started: 27 May 2026

https://doi.org/10.1093/jxb/erq095, 2010.

He, J., Cai, H., and Bai, J.: Irrigation scheduling based on CERES-Wheat model for spring wheat production in the Minqin Oasis in Northwest China, Agricultural Water Management, 128, 19–31, https://doi.org/10.1016/j.agwat.2013.06.010, 2013.

Herzog, M., Striker, G. G., Colmer, T. D., and Pedersen, O.: Mechanisms of waterlogging tolerance in wheat – a review of root and shoot physiology, Plant, Cell & Environment, 39, 1068–1086, https://doi.org/10.1111/pce.12676, 2016.

Hijmans, R. J., Lens, I. M. G.-, and Diepen, C. A. van: WOFOST 6.0 : user's guide for the WOFOST 6.0 crop growth simulation model, 1994.

Hu, J., Zhao, X., Gu, L., Liu, P., Zhao, B., Zhang, J., and Ren, B.: The effects of high temperature, drought, and their combined stresses on the photosynthesis and senescence of summer maize, Agricultural Water Management, 289, 108525, https://doi.org/10.1016/j.agwat.2023.108525, 2023.

Hu, T., Zhang, X., Khanal, S., Wilson, R., Leng, G., Toman, E. M., Wang, X., Li, Y., and Zhao, K.: Climate change impacts on crop yields: A review of empirical findings, statistical crop models, and machine learning methods, Environmental Modelling & Software, 179, 106119, https://doi.org/10.1016/j.envsoft.2024.106119, 2024.

Huang, Y., Yu, Y., Zhang, W., Sun, W., Liu, S., Jiang, J., Wu, J., Yu, W., Wang, Y., and Yang, Z.: Agro-C: A biogeophysical model for simulating the carbon budget of agroecosystems, Agricultural and Forest Meteorology, 149, 106–129, https://doi.org/10.1016/j.agrformet.2008.07.013, 2009.

Jiang, P., Cai, F., Zhao, Z.Q., Meng, Y., Gao, L.Y., and Zhao, T.H.: Physiological and Dry Matter Characteristics of Spring Maize in Northeast China under Drought Stress, Water, 10, 1561, https://doi.org/10.3390/w10111561, 2018.

Jiang, P.: Northeast Corn Material Production and Root Water Absorption Study on the Response of Water Stress, Shenyang Agricultural University, 2019.

Jones, J. W., Hoogenboom, G., Porter, C. H., Boote, K. J., Batchelor, W. D., Hunt, L. A., Wilkens, P. W., Singh, U., Gijsman, A. J., and Ritchie, J. T.: The DSSAT cropping system model, European Journal of Agronomy, 18, 235–265, https://doi.org/10.1016/S1161-0301(02)00107-7, 2003.

Kang, J., Peng, Y., and Xu, W.: Crop Root Responses to Drought Stress: Molecular Mechanisms, Nutrient Regulations, and Interactions with Microorganisms in the Rhizosphere, Int J Mol Sci, 23, 9310, https://doi.org/10.3390/ijms23169310, 2022.

Kang, M.-S., Srivastava, P., Song, J.-H., Park, J., Her, Y., Kim, S. M., and Song, I.: Development of a Component-Based Modeling Framework for Agricultural Water-Resource Management, Water, 8, 351, https://doi.org/10.3390/w8080351, 2016.

Keating, B. A., Carberry, P. S., Hammer, G. L., Probert, M. E., Robertson, M. J., Holzworth, D., Huth, N. I., Hargreaves, J. N. G., Meinke, H., Hochman, Z., McLean, G., Verburg, K., Snow, V., Dimes, J. P., Silburn, M., Wang, E., Brown, S., Bristow, K. L., Asseng, S., Chapman, S., McCown, R. L., Freebairn, D. M., and Smith, C. J.: An overview of APSIM, a model

https://doi.org/10.5194/egusphere-2026-2303
Preprint. Discussion started: 27 May 2026

designed for farming systems simulation, European Journal of Agronomy, 18, 267–288, https://doi.org/10.1016/S1161-0301(02)00108-9, 2003.

Khatun, M., Sarkar, S., Era, F. M., Islam, A. K. M. M., Anwar, M. P., Fahad, S., Datta, R., and Islam, A. K. M. A.: Drought Stress in Grain Legumes: Effects, Tolerance Mechanisms and Management, Agronomy, 11, 2374, https://doi.org/10.3390/agronomy11122374, 2021.

Lesk, C., Rowhani, P., and Ramankutty, N.: Influence of extreme weather disasters on global crop production, Nature, 529, 84–87, https://doi.org/10.1038/nature16467, 2016.

Li, H., Qiu, J., Wang, L., and Yang, L.: Advance in a terrestrial biogeochemical model—DNDC model, Acta Ecologica Sinica, 31, 91–96, https://doi.org/10.1016/j.chnaes.2010.11.006, 2011.

Li, T., Hasegawa, T., Yin, X., Zhu, Y., Boote, K., Adam, M., Bregaglio, S., Buis, S., Confalonieri, R., Fumoto, T., Gaydon, D., Marcaida III, M., Nakagawa, H., Oriol, P., Ruane, A. C., Ruget, F., Singh, B.-, Singh, U., Tang, L., Tao, F., Wilkens, P., Yoshida, H., Zhang, Z., and Bouman, B.: Uncertainties in predicting rice yield by current crop models under a wide range of climatic conditions, Global Change Biology, 21, 1328–1341, https://doi.org/10.1111/gcb.12758, 2015.

Li, Y., Wang, Q., Gao, S., Wang, X., He, A., and He, P.: Effects of Water–Nitrogen Coupling on Root Distribution and Yield of Summer Maize at Different Growth Stages, Plants, 14, 1278, https://doi.org/10.3390/plants14091278, 2025.

Lidon, Z.: An overview on drought induced changes in plant growth, water relationsand photosynthesis, Emir. J. Food Agric, 24, 57, https://doi.org/10.9755/ejfa.v24i1.10599, 2012.

Liu, Z., Zhu, K., Dong, S., Liu, P., Zhao, B., and Zhang, J.: Effects of integrated agronomic practices management on root growth and development of summer maize, European Journal of Agronomy, 84, 140–151, https://doi.org/10.1016/j.eja.2016.12.006, 2017.

Lu, H., Xia, Z., Fu, Y., Wang, Q., Xue, J., and Chu, J.: Response of Soil Temperature, Moisture, and Spring Maize (Zea mays L.) Root/Shoot Growth to Different Mulching Materials in Semi-Arid Areas of Northwest China, Agronomy, 10, 453, https://doi.org/10.3390/agronomy10040453, 2020.

Lynch, J. P., Chimungu, J. G., and Brown, K. M.: Root anatomical phenes associated with water acquisition from drying soil: targets for crop improvement, J Exp Bot, 65, 6155–6166, https://doi.org/10.1093/jxb/eru162, 2014.

Ma, Y., Ren, J., Yang, S., Ding, R., Du, T., Kang, S., and Tong, L.: Enhancing maize yield and water productivity through coordinated root-shoot growth under mild water stress in dense planting, Field Crops Research, 323, 109786, https://doi.org/10.1016/j.fcr.2025.109786, 2025.

Manghwar, H., Hussain, A., Alam, I., Khoso, M. A., Ali, Q., and Liu, F.: Waterlogging stress in plants: Unraveling the mechanisms and impacts on growth, development, and productivity, Environmental and Experimental Botany, 224, 105824, https://doi.org/10.1016/j.envexpbot.2024.105824, 2024.

McCown, R. L., Hammer, G. L., Hargreaves, J. N. G., Holzworth, D. P., and Freebairn, D. M.:

https://doi.org/10.5194/egusphere-2026-2303
Preprint. Discussion started: 27 May 2026

APSIM: a novel software system for model development, model testing and simulation in agricultural systems research, Agricultural Systems, 50, 255–271, https://doi.org/10.1016/0308-521X(94)00055-V, 1996.

Monteleone, B., Borzí, I., Arosio, M., Cesarini, L., Bonaccorso, B., and Martina, M.: Modelling the response of wheat yield to stage-specific water stress in the Po Plain, Agricultural Water Management, 287, 108444, https://doi.org/10.1016/j.agwat.2023.108444, 2023.

Munns, R. and Tester, M.: Mechanisms of Salinity Tolerance, Annu. Rev. Plant Biol., 59, 651–681, https://doi.org/10.1146/annurev.arplant.59.032607.092911, 2008.

Núñez, A., Ball, R., and Schipanski, M.: Plant and soil microbial responses to irrigation retirement in semiarid cropping systems, Environ. Res. Commun., 4, 035004, https://doi.org/10.1088/2515-7620/ac59c3, 2022.

Novák, V., Hurtalová, T., and Matejka, F.: Predicting the effects of soil water content and soil water potential on transpiration of maize, Agricultural Water Management, 76, 211–223, https://doi.org/10.1016/j.agwat.2005.01.009, 2005.

Oktem, A.: Effect of water shortage on yield, and protein and mineral compositions of drip-irrigated sweet corn in sustainable agricultural systems, Agricultural Water Management, 95, 1003–1010, https://doi.org/10.1016/j.agwat.2008.03.006, 2008.

Palta, J. A., Kobata, T., Turner, N. C., and Fillery, I. R.: Remobilization of Carbon and Nitrogen in Wheat as Influenced by Postanthesis Water Deficits, Crop Science, 34, 118–124, https://doi.org/10.2135/cropsci1994.0011183X003400010021x, 1994.

Pasley, H. R., Huber, I., Castellano, M. J., and Archontoulis, S. V.: Modeling Flood-Induced Stress in Soybeans, Front. Plant Sci., 11, 62, https://doi.org/10.3389/fpls.2020.00062, 2020.

Pouri, K., Mardeh, A. S.-S., Sohrabi, Y., and Soltani, A.: Crop phenotyping for wheat yield and yield components against drought stress, Cereal Research Communications, 47, 383–393, https://doi.org/10.1556/0806.47.2019.05, 2019.

Priestley, C. H. B. and Taylor, R. J.: On the Assessment of Surface Heat Flux and Evaporation Using Large-Scale Parameters, 1972.

Protto, V., Bauget, F., Rishmawi, L., Nacry, P., and Maurel, C.: Primary, seminal and lateral roots of maize show type-specific growth and hydraulic responses to water deficit, Plant Physiology, 194, 2564–2579, https://doi.org/10.1093/plphys/kiad675, 2024.

Rishmawi, L., Bauget, F., Protto, V., Bauland, C., Nacry, P., and Maurel, C.: Natural variation of maize root hydraulic architecture underlies highly diverse water uptake capacities, Plant Physiology, 192, 2404–2418, https://doi.org/10.1093/plphys/kiad213, 2023.

Ritchie, J. T.: Soil water balance and plant water stress, in: Understanding Options for Agricultural Production, edited by: Tsuji, G. Y., Hoogenboom, G., and Thornton, P. K., Springer Netherlands, Dordrecht, 41–54, https://doi.org/10.1007/978-94-017-3624-4_3, 1998.

Saseendran, S. a., Ahuja, L. r., Ma, L., and Trout, T. j.: Modeling for Best Management of the Effects of Irrigation Frequencies, Initial Water, and Nitrogen on Corn, in: Practical

https://doi.org/10.5194/egusphere-2026-2303
Preprint. Discussion started: 27 May 2026

Applications of Agricultural System Models to Optimize the Use of Limited Water, John Wiley & Sons, Ltd, 25–52, https://doi.org/10.2134/advagricsystmodel5.c2, 2014.

Saxton, K. E. and Rawls, W. J.: Soil Water Characteristic Estimates by Texture and Organic Matter for Hydrologic Solutions, Soil Science Soc of Amer J, 70, 1569–1578, https://doi.org/10.2136/sssaj2005.0117, 2006.

Seleiman, M. F., Al-Suhaibani, N., Ali, N., Akmal, M., Alotaibi, M., Refay, Y., Dindaroglu, T., Abdul-Wajid, H. H., and Battaglia, M. L.: Drought Stress Impacts on Plants and Different Approaches to Alleviate Its Adverse Effects, Plants, 10, 259, https://doi.org/10.3390/plants10020259, 2021.

Shao, G. C., Lan, J. J., Yu, S. E., Liu, N., Guo, R. Q., and She, D. L.: Photosynthesis and growth of winter wheat in response to waterlogging at different growth stages, Photosynthetica, 51, 429–437, https://doi.org/10.1007/s11099-013-0039-9, 2013.

Smith, M. R., Rao, I. M., and Merchant, A.: Source-Sink Relationships in Crop Plants and Their Influence on Yield Development and Nutritional Quality, Front. Plant Sci., 9, https://doi.org/10.3389/fpls.2018.01889, 2018.

Steduto, P., Hsiao, T. C., Raes, D., and Fereres, E.: AquaCrop—The FAO Crop Model to Simulate Yield Response to Water: I. Concepts and Underlying Principles, Agronomy Journal, 101, 426–437, https://doi.org/10.2134/agronj2008.0139s, 2009.

Stöckle, C. O., Donatelli, M., and Nelson, R.: CropSyst, a cropping systems simulation model, European Journal of Agronomy, 18, 289–307, https://doi.org/10.1016/S1161-0301(02)00109-0, 2003.

Tsuji, G. Y.: Understanding Options for Agricultural Production, 1st ed., Springer Netherlands, Dordrecht, 1 pp., 1998.

Vadez, V., Grondin, A., Chenu, K., Henry, A., Laplaze, L., Millet, E. J., and Carminati, A.: Crop traits and production under drought, Nat Rev Earth Environ, 5, 211–225, https://doi.org/10.1038/s43017-023-00514-w, 2024.

Vicente-Serrano, S. M., Peña-Angulo, D., Beguería, S., Domínguez-Castro, F., Tomás-Burguera, M., Noguera, I., Gimeno-Sotelo, L., and El Kenawy, A.: Global drought trends and future projections, Phil. Trans. R. Soc. A., 380, 20210285, https://doi.org/10.1098/rsta.2021.0285, 2022.

Wang, C., Liu, W., Li, Q., Ma, D., Lu, H., Feng, W., Xie, Y., Zhu, Y., and Guo, T.: Effects of different irrigation and nitrogen regimes on root growth and its correlation with above-ground plant parts in high-yielding wheat under field conditions, Field Crops Research, 165, 138–149, https://doi.org/10.1016/j.fcr.2014.04.011, 2014.

Wang, G., Huang, Y., Zhang, W., Yu, Y., and Sun, W.: Quantifying carbon input for targeted soil organic carbon sequestration in China's croplands, Plant Soil, 394, 57–71, https://doi.org/10.1007/s11104-015-2508-3, 2015.

Wang, L., Liu, X., Liu, X., Bao, X., Zhang, X., Yin, B., Wang, W., Wang, Y., and Zhen, W.: Effects of spring limited irrigation on grain yield and root characteristics of winter wheat in groundwater-overexploitation areas in the North China Plain, Agricultural Water

https://doi.org/10.5194/egusphere-2026-2303
Preprint. Discussion started: 27 May 2026

Management, 294, 108729, https://doi.org/10.1016/j.agwat.2024.108729, 2024.

Wang, Y.:. Study on the relationship among root system and shoot dry matter accumulation and yield from winter wheat under different cultivation and management modes, Henan Agricultural University, 2011

Wang, Y.: Studies on Formation of Root Configuration and Its Relationships to Utilization of Water and Nitrogen Fertilizers and Grain Yield in Winter Wheat (Triticum aestivum L.) under Different Cultivation Management Patterns, Henan Agricultural University, 2014.

Wolf, J.: Calibration of WOFOST crop growth simulation model for use within CGMS, n.d.

Xu, H., Vandecasteele, B., Maenhout, P., Pannecoucque, J., De Neve, S., and Sleutel, S.: Maize root biomass and architecture depend on site but not on variety: Consequences for prediction of C inputs and spread in topsoil based on root-to-shoot ratios, European Journal of Agronomy, 119, 126121, https://doi.org/10.1016/j.eja.2020.126121, 2020.

Xu, W., Zhang, W., Yu, Y., Sun, W., Yu, L., Shang, D., Xue, C., and Zhang, Q.: Response of crop photosynthetic product allocation under different water supply conditions: A global synthetic analysis, Field Crops Research, 333, 110104, https://doi.org/10.1016/j.fcr.2025.110104, 2025.

Xu, W., Zhang, W., Yu, Y., & Zhang, Q.: Optimization code of Agro-C water module and photosynthetic product allocation module. In Improving photo (1.0), Zenodo. https://doi.org/10.5281/zenodo.19970992, 2026

Xue, Q., Zhu, Z., Musick, J. T., Stewart, B. A., and Dusek, D. A.: Root growth and water uptake in winter wheat under deficit irrigation, Plant and Soil, 257, 151–161, https://doi.org/10.1023/A:1026230527597, 2003.

Yan, Z., Liu, Y., Gao, S., Yang, H., Feng, D., Gao, K., Ming, B., Wang, K., Hou, P., Li, S., and Xie, R.: Water management mitigates drought stress effects on maize leaf senescence and post-anthesis dry matter accumulation, Agricultural Water Management, 318, 109709, https://doi.org/10.1016/j.agwat.2025.109709, 2025.

Yang, Y., Ma, X., Yan, L., Li, Y., Wei, S., Teng, Z., Zhang, H., Tang, W., Peng, S., and Li, Y.: Soil–root interface hydraulic conductance determines responses of photosynthesis to drought in rice and wheat, Plant Physiology, 194, 376–390, https://doi.org/10.1093/plphys/kiad498, 2023.

Yu, Y., Huang, Y., and Zhang, W.: Changes in rice yields in China since 1980 associated with cultivar improvement, climate and crop management, Field Crops Research, 136, 65–75, https://doi.org/10.1016/j.fcr.2012.07.021, 2012.

Zeitoun, M., Lankford, B., Krueger, T., Forsyth, T., Carter, R., Hoekstra, A. Y., Taylor, R., Varis, O., Cleaver, F., Boelens, R., Swatuk, L., Tickner, D., Scott, C. A., Mirumachi, N., and Matthews, N.: Reductionist and integrative research approaches to complex water security policy challenges, Global Environmental Change, 39, 143–154, https://doi.org/10.1016/j.gloenvcha.2016.04.010, 2016.

Zhao, J., Xue, Q., Jessup, K. E., Hou, X., Hao, B., Marek, T. H., Xu, W., Evett, S. R., O'Shaughnessy, S. A., and Brauer, D. K.: Shoot and root traits in drought tolerant maize (Zea

https://doi.org/10.5194/egusphere-2026-2303
Preprint. Discussion started: 27 May 2026

mays L.) hybrids, Journal of Integrative Agriculture, 17, 1093–1105, https://doi.org/10.1016/S2095-3119(17)61869-0, 2018.

Zhang, Q., Zhang, W., Li, T., Sun, W., Yu, Y., and Wang, G.: Projective analysis of staple food crop productivity in adaptation to future climate change in China, Int J Biometeorol, 61, 1445–1460, https://doi.org/10.1007/s00484-017-1322-4, 2017.

Zhang, X.: Effects of Different Water-Nitrogen Treatments on Root Growth and the Accumulation and Translocation of Aboveground Dry Matter together with Yield in Wheat, Henan Agricultural University, 2023.

Zhou, D., Wang, H., Wang, X., Wang, F., Zhang, J., and Ma, D.: Evaluation of AquaCrop's Ability to Simulate Water Stress Based on 2-Year Case Study of Maize Crop, Agronomy, 14, 354, https://doi.org/10.3390/agronomy14020354, 2024.

Zlatev, Z. and Lidon, F.: An overview on drought induced changes in plant growth, water relations and photosynthesis, Emirates Journal of Food and Agriculture, 24, 2012

Zou, Y., Saddique, Q., Ali, A., Xu, J., Khan, M. I., Qing, M., ... & Siddique, K. H.: Deficit irrigation improves maize yield and water use efficiency in a semi-arid environment, Agricultural Water Management, 243, 106483, 2021.